area influenced by the coastal stations is mostly in the south and comprises 10.5% of the ice sheet area, and accounted for -38.5 km^3/year volume change (75% of the total). The true volume change in this area is likely to be greater.

13. R. Warrick, C. Le Provost, M. Meier, J. Oerlemans, P. Woodworth, in *Climate Change, 1995: The Science of Climate Change* (Cambridge Univ. Press, Cambridge, 1996), pp. 359–405.
14. Temperature records were decoded by the National Center for Environmental Prediction and were obtained from the National Center for Atmospheric Research.
15. M. M. Herron, S. L. Herron, C. C. Langway, *Nature* **293**, 389 (1981).
16. A temperature record for 1900–95 was calculated using data from the NOAA National Climate Diagnostic Center accessible at http://www.ncdc.noaa.gov/onlineprod/ghcnmcdwseasonal/form.html. Quality control procedures are described in J. K. Eischeid *et al.* [*J. Appl. Meteorol.* **34**, 2787 (1995)].
17. A. Weidick, *Rapp. Gronlands Geol. Unders.* **152**, 73 (1991).

18. We thank the crew of the NASA P-3 aircraft used for the Greenland surveys. We acknowledge the technical support of R. Mitchell, A. Waller, and J. Scott. This work was supported by NASA's Polar Research Program and the ICESAT Project.

2 March 2000; accepted 7 June 2000

Stability of Ferropericlase in the Lower Mantle

L. S. Dubrovinsky,[1]* N. A. Dubrovinskaia,[1] S. K. Saxena,[1] H. Annersten,[1] E. Hålenius,[1] H. Harryson,[1] F. Tutti,[1] S. Rekhi,[1] T. Le Bihan[2]

We have heated ferropericlases $(Mg_{0.60}Fe_{0.40})O$ and $(Mg_{0.50}Fe_{0.50})O$ to temperatures of 1000 kelvin at pressures of 86 gigapascals, simulating the stability of the solid solution at physical conditions relevant to Earth's lower mantle. The in situ x-ray study of the externally heated samples in a Mao-Bell–type diamond anvil cell shows that ferropericlase may dissociate into magnesium-rich and iron-rich oxide components. The result is important because the decomposition of ferropericlase into lighter and heavier phases will cause dynamic effects that could lead to mantle heterogeneity.

Ferropericlase (Mg,Fe)O and $(Mg,Fe)SiO_3$-perovskite are considered to form the bulk of Earth's lower mantle. Therefore, ferropericlase [$(Mg_{1-x}Fe_x)O$, $x \leq 0.5$] and magnesiowüstite [$(Mg_{1-x}Fe_x)O$, $x > 0.5$] have been studied extensively (*1–14*). At ambient conditions, the end members of the MgO-FeO solid solution—periclase (MgO) and wüstite (FeO)—have the same halite NaCl (B1) structure, and they form a complete solid solution. However, at pressures above 17 GPa and ambient temperature (*15*), wüstite transforms to a phase with rhombohedral structure (*16*). With increasing pressure above 100 GPa at 300 K, it transforms to the NiAs (B8) or the anti-NiAs (a-B8) structure (*7, 12, 13*), whereas periclase retains the NaCl structure at least to 227 GPa (*11*). The NaCl structure is based on cubic close packing of the anions, but the B8 (or the a-B8) structure is formed by hexagonal close packing of the anions (or cations). The topological difference between the B8 and B1 structures at high pressure could lead to an immiscibility gap in the region of the MgO-FeO solid solution (*17*). To investigate this hypothesis, we conducted an in situ high-pressure, high-temperature study of ferropericlase with two intermediate compositions, $(Mg_{0.6}Fe_{0.4})O$ and quenched $(Mg_{0.5}Fe_{0.5})O$, respectively.

Experiments were performed on beamline ID30 at ESRF (Grenoble, France) and at the Uppsala Lab in Sweden (*18*). Samples, synthesized as described in (*1*), were externally heated in a Mao-Bell–type diamond anvil cell (*15*). The powder samples of ferropericlase were loaded into a hole (initial diameter 70 to 75 μm) in a Re gasket, which was then confined between beveled diamonds with 200-μm culets. Pressure was determined by using powdered platinum (99.999% purity) as an in situ x-ray standard mixed in small proportion (~5 volume %) with the ferropericlase samples. For the analysis of the integrated x-ray spectra, we used the programs GSAS (*19*) and PeakFit 4.0 (Figs. 1 and 2). The lattice parameter of Pt was determined with a precision better than 0.002 Å over the whole pressure and temperature range studied, resulting in an uncertainty of 2 GPa at pressures up to 80 GPa. At ambient conditions, the lattice parameters of ferropericlase are 4.2627(6) Å (numbers in parentheses are standard deviations in the last significant digits) for $(Mg_{0.6}Fe_{0.4})O$ and 4.2716(7) Å for $(Mg_{0.5}Fe_{0.5})O$. These values agree with previous data (*1, 2, 4*). Rietveld refinements yielded occupancies for the metal position of Fe 0.38(3) and Mg 0.62(3) in $(Mg_{0.6}Fe_{0.4})O$ and Fe 0.52(4) and Mg 0.48(4) in $(Mg_{0.5}Fe_{0.5})O$.

In our experiments with ferropericlase $(Mg_{0.6}Fe_{0.4})O$, we first increased the pressure at ambient temperature to 47 ± 1 GPa (*15*) (Fig. 1) and then increased the temperature to 950 to 980 K. This heating further raised the pressure to 61 ± 2 GPa. The sample was heated for 4 hours, during which no changes were observed except for a slight asymmetric broadening of the (220) reflection. Then the pressure was increased to 86 ± 2 GPa at a temperature of 975 ± 5 K (*15*), and after 5 to 6 hours of heating, all the reflections of ferropericlase became asymmetric and some showed splitting (Figs. 1 to 3). It was not possible to describe the diffraction pattern assuming only a mixture of cubic ferropericlase and platinum (Fig. 2A). A mixture of three phases [platinum, cubic, and rhombohedral ferropericlases in the proportion 1:22:3 (Fig. 2B)] had to be assumed to reproduce all features of the pattern. Cubic ferropericlase (Fig. 2B) had a molar volume of 8.68(1) cm^3/mol, corresponding to a pressure of 84 ± 2 GPa at 970 K according to the equation of state for $(Mg_{0.6}Fe_{0.4})O$ (*4*). The molar volume of the rhombohedral phase (Fig. 2B) at the same condition is 9.20(1) cm^3/mol. The thermal equation of state of rhombohedral ferropericlase is unknown. Using available data (*4, 5, 16*), we estimated the bulk modulus at ambient conditions, $K_{300,0}$, to lie between 150 and 160 GPa, its pressure derivative $K' = 4$, and dK/dT between -0.01 and -0.025 GPa/K. The observed molar volume V_0 of 9.20 cm^3/mol at 85 GPa and 970 K would indicate a molar volume of 12.14 to 12.31 cm^3/mol at ambient conditions. These values correspond to the volume of stoichiometric cubic wüstite (*2, 20*). Upon decompression, the reflections of ferropericlase remained split (Fig. 1). The quality of the diffraction patterns of the quenched samples was not good enough for Rietveld refinement, but the x-ray data of the quenched samples at ambient conditions showed the presence of two cubic phases with lattice parameters of 4.253(1) and 4.327(1) Å, respectively. The first corresponds to a ferropericlase with the composition 35 atomic % FeO and 65 atomic % MgO, and the second to an almost stoichiometric pure wüstite (*2, 20*). The lattice parameters of platinum matched the initial value before the experiments [$a = 3.9231(5)$ Å] within experimental error (0.0004 Å). Within the limit of error (~3%), no ferric iron was detected by Mössbauer spectroscopy in the ferropericlase before and after our experiments (*21*).

In the experiments with ferropericlase $(Mg_{0.5}Fe_{0.5})O$, we heated the sample for 5 to 6 hours between 950 and 1000 K at four different pressures: 56(3), 67(3), 74(4), and 83(5) GPa

---

[1] Institute of Earth Sciences, Uppsala University, S-752 36 Uppsala, Sweden. [2] European Synchrotron Radiation Facility (ESRF), BP 220, F-38043 Grenoble Cedex, France.

*To whom correspondence should be addressed.

(Fig. 3B) (*15*). After heating at each pressure, the sample was quenched and studied by x-ray and Mössbauer spectroscopy. Heating at pressures up to 74(4) GPa did not show any changes after quenching, but heating at 83(5) GPa demonstrated a splitting of the ferropericlase reflections, indicating two cubic phases with lattice parameters 4.237(3) Å and 4.325(2) Å. Similar to $(Mg_{0.6}Fe_{0.4})O$, the larger lattice parameter of the sample $(Mg_{0.5}Fe_{0.5})O$ corresponds to an almost stoichiometric pure wüstite, whereas the smaller lattice parameter could be estimated with the composition 20% FeO and 80% MgO (*2, 20*). Mössbauer measurements before heating and on quenched materials did not detect ferric iron or the appearance of any non-wüstite phase (*21*). Recovered samples were also studied by electron microprobe analysis (*22*). The starting material and the materials heated at pressures up to 74(4) GPa were homogeneous and had composition $Fe_{0.504(9)}Mg_{0.496(7)}O$. But after heating at 83(5) GPa, the recovered sample was not homogeneous and contained particles with almost pure wüstite composition $Fe_{0.985(10)}Mg_{0.001(2)}O$ (black spots on inset, Fig. 3B). Magnesium-rich parts of the sample with average composition $Fe_{0.211(10)}Mg_{0.789(17)}O$ was inhomogeneous on the submicrometer level (small white spots in gray matrix, inset, Fig. 3B).

Fig. 1. Sequence (from bottom to top) of diffraction patterns collected during compression and heating of ferropericlase. Arrows show broad and split reflections of ferropericlase/wüstite.

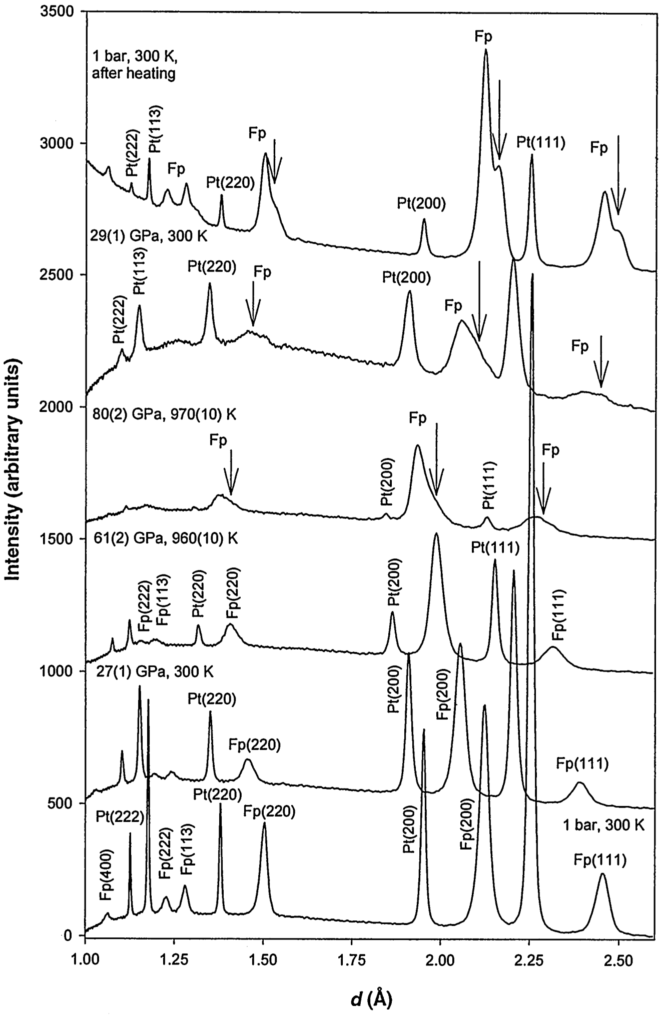

We did not observe the formation of a B8 or anti-B8 modification of FeO, although the conditions of our experiment are close to the transition at 85 GPa above 800 K as proposed by Fei and Mao (*7*). There could be several reasons for such a difference in observations: (i) The composition of wüstite could influence the position of the phase boundary, (ii) a small amount of MgO in wüstite might stabilize the rhombohedral phase with respect to B8 or anti-B8, or (iii) a small amount of MgO in wüstite might promote decomposition of the rhombohedral phase forming metastably. The decomposition of the intermediate ferropericlases at pressures greater than 85 GPa may suggest that the driving force of the process is either the transition of cubic wüstite to the NiAs-type structure or possible changes in the magnetic structure of Fe^{2+} (*14*).

We cannot resolve the question of the

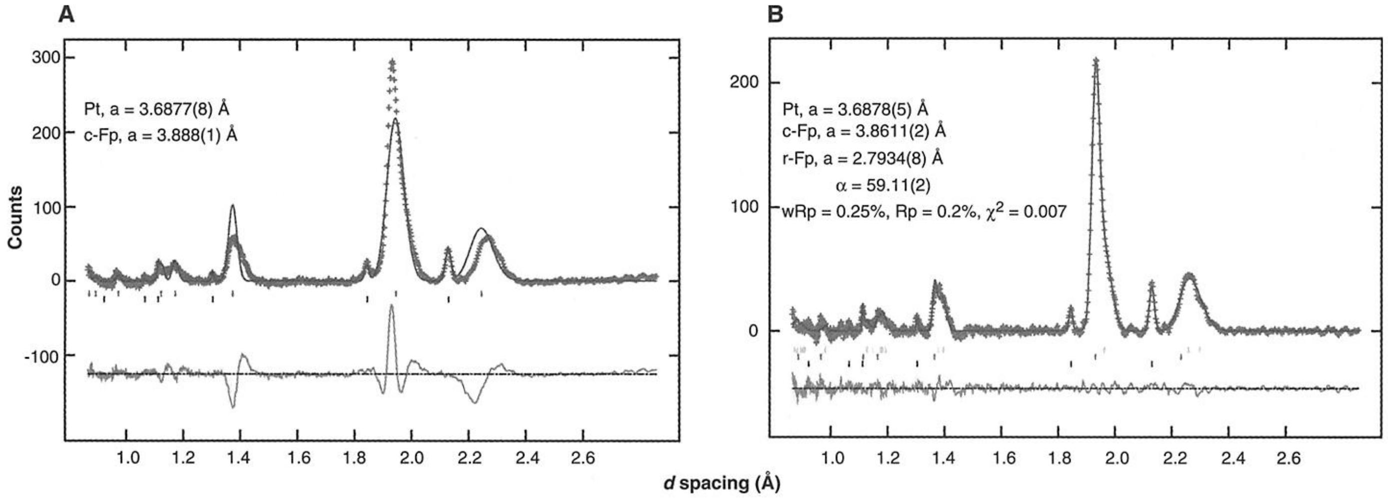

Fig. 2. Example of analyzed integrated patterns of the spectrum collected at 970(10) K and 86(2) GPa after 6 hours of heating. It is not possible to describe the diffraction pattern in terms of a mixture of cubic ferropericlase (c-Fp) and platinum (**A**), but a mixture of three phases—platinum, cubic, and rhombohedral (r-Fp) ferropericlases (**B**)—perfectly reproduces all features of the pattern. The GSAS program package was used. The background was subtracted (*19*).

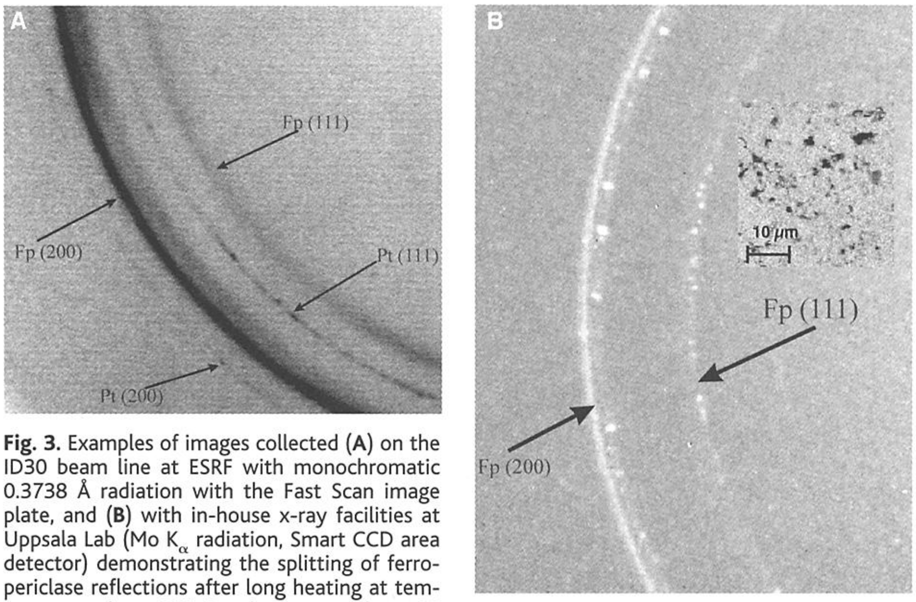

Fig. 3. Examples of images collected (**A**) on the ID30 beam line at ESRF with monochromatic 0.3738 Å radiation with the Fast Scan image plate, and (**B**) with in-house x-ray facilities at Uppsala Lab (Mo K_α radiation, Smart CCD area detector) demonstrating the splitting of ferropericlase reflections after long heating at temperatures above 950 K and pressures above 80 GPa. Inset shows backscattered electron image of the recovered sample (black, iron-rich parts; white, magnesium-rich parts).

width of the immiscibility gap in the MgO-FeO system at high pressure, nor can we determine whether ferropericlase might dissociate completely into MgO and FeO after a sufficiently long time of heating. However, the ferropericlases at least partially dissociate into a phase with lower density (Mg-rich, ~6.1 g/cm^3) and a phase with higher density (Fe-rich, ~7.8 g/cm^3) at 85 GPa, corresponding to a depth of 1900 to 2000 km (Preliminary Reference Earth Model). Such dissociation of ferropericlase along with phase transitions in silica (*23*) and possible dissociation of (Mg,Fe)SiO$_3$-perovskite (*10*, *17*, *23*) may lead to the heterogeneity of the lower mantle.

References and Notes

1. M. Rosenhauer, H. K. Mao, E. Woermann, *Yearb. Carnegie Inst. Washington* **75**, 513 (1976).
2. P. Richet, H. K. Mao, P. M. Bell, *J. Geophys. Res.* **94**, 3037 (1989).
3. D. G. Isaak, R. E. Cohen, M. J. Mehl, *J. Geophys. Res.* **95**, 7055 (1990).
4. Y. Fei, H. K. Mao, J. Shu, J. Hu, *Phys. Chem. Miner.* **18**, 416 (1992).
5. Y. Fei, *Am. Mineral.* **84**, 272 (1999).
6. ———, *Geochem. Soc. Spec. Pub. 243* (1996).
7. ——— and H. K. Mao, *Science* **266**, 1678 (1994).
8. M. P. Pasternak *et al.*, *Phys. Rev. Lett.* **79**, 5046 (1997).
9. R. E. Cohen, in *Review of High-Pressure Science and Technology*, M. Nakahara, Ed. (AIP Press, Kyoto, Japan, 1998), vol. 7, p. 160.
10. H. K. Mao, G. Shen, R. J. Hemley, *Science* **278**, 2098 (1997).
11. T. S. Duffy, R. J. Hemley, H. K. Mao, *Phys. Rev. Lett.* **74**, 1371 (1995).
12. Z. Fang, K. Terakura, H. Sawada, T. Miyazaki, I. Solovyev, *Phys. Rev. Lett.* **81**, 1027 (1998).
13. I. I. Mazin, Y. Fei, R. Downs, R. E. Cohen, *Mineralogy* **83**, 451 (1998).
14. R. E. Cohen, I. I. Mazin, D. G. Isaak, *Science* **275**, 654 (1997).
15. See *Science* Online (www.sciencemag.org/feature/data/1050995.shl).
16. J. Shu, H. K. Mao, J. Hu, Y. Fei, R. J. Hemley, *N. Jb. Mineral. Abh.* **172**, 309 (1998).
17. C. A. McCammon, A. E. Ringwood, I. Jackson, *Geophys. J. R. Astron. Soc.* **72**, 577 (1983).
18. At Uppsala Lab we have obtained powder x-ray diffraction data with a Siemens x-ray system consisting of a Smart charge-coupled device (CCD) area detector and a direct-drive rotating anode as x-ray generator (18 kW). The Mo K_α radiation (tube voltage 50 kV, tube current 24 mA, cathode gun 0.1 × 1 mm) is focused with a capillary x-ray optical system to 40 μm full width at half-maximum. At ESRF we collected the powder diffraction data with a fine incident x-ray beam (approximately rectangular shape with dimensions 8 μm by 9 μm or less) of wavelength 0.3738 Å on the FastScan imaging plate. The collected images were integrated to obtain conventional diffraction spectra.
19. A. C. Larson and R. B. Von Dreele, *GSAS (General Structure Analysis System) LANSCE, MS-H805* (Los Alamos National Laboratory, Los Alamos, NM, 1994), p. 86.
20. S. Stolen, R. Glokner, F. Gronvold, T. Atake, S. Izumisawa, *Am. Mineral.* **81**, 973 (1996).
21. E. Hålenius, H. Annersten, S. Jönsson, *Geochem. Soc. Spec. Pub. 5* (1996), p. 255. Mössbauer experiments were performed using a conventional transmission geometry. Measurements were made on the quenched samples mounted on the diamond and leading the gamma rays through the gasket hole. A point source of ^{57}Co in Rh, nominal value 60 mCi, was used in the experiment and calibrated against α-Fe at room temperature.
22. Chemical analyses were obtained using the CAMEBAX SX-50 electron microprobe with a phi-rho-Z correction procedure (operating conditions: accelerating potential, 20 kV; beam current, 50 nA; beam diameter, 1 to 2 μm). Counting times were 10 s. The following analyzing crystals were used: TAP for Mg K_α, Al K_α, and Si K_α; LiF for Mn K_α and Fe K_α.
23. S. K. Saxena, P. Lazor, L. S. Dubrovinsky, *Mineral. Petrol.* **69**, 1 (2000).
24. Supported by the Swedish Natural Science Council and the Wallenberg and Crafoords Funds. The synchrotron x-ray studies were conducted at ESRF, Grenoble, on the ID30 beam line. The comments of two anonymous referees were useful.

6 March 2000; accepted 30 May 2000

Pattern of Marine Mass Extinction Near the Permian-Triassic Boundary in South China

Y. G. Jin,[1]* Y. Wang,[1] W. Wang,[1] Q. H. Shang,[1] C. Q. Cao,[1] D. H. Erwin[2]

The Meishan section across the Permian-Triassic boundary in South China is the most thoroughly investigated in the world. A statistical analysis of the occurrences of 162 genera and 333 species confirms a sudden extinction event at 251.4 million years ago, coincident with a dramatic depletion of $\delta^{13}C_{carbonate}$ and an increase in microspherules.

The end-Permian mass extinction eliminated over 90% of all marine species and had a significant impact on land species as well (*1*, *2*). However, geochronologic results from South China reveal that the main extinction occurred over a period of less than 500,000 years (*3*), coincident with the eruption of the Siberian flood basalts (*4*, *5*) and with a sharp shift in $\delta^{13}C_{carb}$ (*6*). Although there are claims for multiple pulses of extinction, including at least three at the classic Meishan sections in South China (*7*, *8*) [probably the most thoroughly studied Permian-Triassic (P-T) marine boundary section in the world], the cause of the extinction remains enigmatic. Here we examine sampling and preservation effects (*9*) using a statistical analysis of species' stratigraphic ranges (*10*, *11*) to demonstrate the extreme rapidity of the extinction.

---

[1] Nanjing Institute of Geology and Palaeontology, Academia Sinica, Nanjing 210008, China. [2] Department of Paleobiology, MRC-121, National Museum of Natural History, Washington, DC 20560, USA.

*To whom correspondence should be addressed. E-mail: ygjin@public1.ptt.js.cn